Chapter 10
Model Complexity of Distributed Parameter Systems: An Energy-Based Approach

L.S. Louca

10.1 Introduction

Modeling and simulation have yet to achieve wide utilization as commonplace engineering tools. One reason for this is that current modeling and simulation techniques are inadequate. Specifically, a major disadvantage is that they require sophisticated users who are often not domain experts and thus lack the ability to effectively utilize the model and simulation tools to uncover the important design trade-offs. Another drawback is that models are often large and complicated with many parameters, making the physical interpretation of the model outputs, even by domain experts, difficult. This is particularly true when "unnecessary" features are included in the model.

A variety of algorithms have been developed and implemented to help automate the production of proper models of dynamic systems. Wilson and Stein developed Model Order Deduction Algorithm (MODA) that deduces the required system model complexity from subsystem models of variable complexity using a frequency-based metric [25]. They also defined proper models as the models with physically meaningful states and parameters that are of necessary but sufficient complexity to meet the engineering and accuracy objectives. Additional work on deduction algorithms for generating proper models in an automated fashion has been reported by previous research [4, 5, 24]. The above algorithms have also been implemented in an automated modeling computer environment [22].

In an attempt to overcome the limitations of the frequency-based metrics, the author introduced a new model reduction technique that also generates proper models [16]. This approach uses an energy-based metric (element activity) that

L.S. Louca (✉)
Department of Mechanical and Manufacturing Engineering, University of Cyprus, Nicosia 1678, Cyprus
e-mail: lslouca@ucy.ac.cy

W. Borutzky (ed.), *Bond Graphs for Modelling, Control and Fault Diagnosis of Engineering Systems*, DOI 10.1007/978-3-319-47434-2_10

in general can be applied to nonlinear systems, and considers the importance of all energetic elements (generalized inductance, capacitance, and resistance) [17]. The contribution of each energy element in the model is ranked according to the activity metric under specific excitation. Elements with small contributions are eliminated in order to produce a reduced model using a systematic methodology called Model Order Reduction Algorithm (MORA). The activity metric was also used as a basis for even further reduction, through partitioning the model into smaller and decoupled submodels [19].

Such modeling approaches should be able to handle real mechanical systems that typically include distributed parameter (continuous) components, e.g., rods, beams, plates, etc. Frequently, modeling objectives and assumptions allow the lumping of continuous component properties into ideal energy elements that lead to a dynamic model described by a set of ordinary differential equations. However, when property lumping is not acceptable, modeling of a continuous component requires a different approach since its inertial, compliance, and resistive properties are spatially distributed and cannot be lumped into single equivalent elements. The dynamic behavior of continuous components is thus described by partial differential equations with derivatives in both time and space. Another approach that is considered in this work is the modeling of a continuous component with finite segments that are spatially distributed. This is an approximation for which the accuracy is a function of the number of segments. The model accuracy improves as the number of segments increases. Model accuracy and the required number of segments can be addressed using a frequency-based metric [5].

Beyond the physical-based modeling, modal decomposition is also used to model and analyze continuous and discrete systems [18]. One of the advantages of modal decomposition is the ability to straightforwardly adjust (i.e., reduce) model complexity since all modes are orthogonal to each other. The reduction of such modal decomposition models is mostly based on frequency, and the user-defined Frequency Range Of Interest (FROI) determines the frequencies that are important for a specific scenario. In this case, modes with frequencies within the FROI are retained in the reduced model and modes outside this range are eliminated. As expected, mode truncation introduces error in the predictions that can be measured and adjusted based on the accuracy requirements [9, 10].

Element activity is another metric that has more flexibility than frequency-based metrics, which address the issue of model complexity by only adding compliant elements, leaving unaccounted the importance of inertial and resistive elements. In contrast, the activity metric considers the importance of all energetic elements, and therefore, the significance of all energy elements in the model can be quantified. It is the purpose of this work to develop a new methodology using the activity metric for addressing the model complexity of distributed parameter systems and specifically cantilever beams. The methodology is specifically developed using the finite segment approximation and the goal is to identify the physical phenomena to be included in each segment in order to accurately predict the dynamic behavior.

The chapter starts with providing background on the energy-based activity metric along with the reduction algorithm. Next, the equation formulation for a finite

segment Timoshenko beam is presented along with the closed form expressions for steady state element activities. Then, the complexity of a cantilever beam is analyzed under various conditions using MORA. Finally, in the last section, discussion and conclusions are provided.

10.2 Background

The original work on the energy-based metric for model reduction is briefly described here for convenience. More details, extensions, and applications of this methodology can be found in previous publications [13–15, 17]. The main idea behind this model reduction technique is to evaluate the "element activity" of individual energy elements in a full system model under a stereotypical set of inputs and initial conditions. The activity of each energy element establishes a hierarchy of importance for all elements in a system. Those below a user-defined threshold of acceptable level of activity are eliminated from the model. A reduced model is then generated and a new set of governing differential equations is derived.

The activity metric has been formulated originally for systems with nonlinearities in both the element constitutive laws and kinematics. In this work, the activity metric is applied to linear systems for which analytical expressions for the activity can be derived, and therefore, avoid the use of numerical time integration that could be cumbersome. The analysis is further simplified if, in addition to the linearity assumption, the system is assumed to have a single sinusoidal excitation, and only the steady state response is studied. These assumptions are motivated from Fourier analysis where an arbitrary function can be decomposed into a series of harmonics. Using this frequency decomposition, the activity analysis can be performed as a function of frequency in order to study the frequency dependency of element activity in a dynamic system.

10.2.1 Element Activity for Linear Systems

A measure of the power response of a dynamic system, which has physical meaning and a simple definition, is used to develop the modeling metric, element activity (or simply "activity"). Element activity, A, is defined for each energy element as:

$$A = \int_0^\tau |\mathbb{P}(t)| \mathrm{d}t \tag{10.1}$$

where $\mathbb{P}(t)$ is the element power and τ is the time over which the model has to accurately predict the system behavior. The activity has units of energy, representing the amount of energy that flows in and out of the element over the given time τ. The energy that flows in and out of an element is a measure of how active this element

is (how much energy passes through it), and consequently the quantity in (10.1) is termed activity. Activity can be defined independent of the energy domain, type of energy element, or nonlinearities.

The activity is calculated for each energy element based on the system response that is calculated from the system's state equations. In the case that the system is modeled using a bond graph formulation, the state equations are derived using the multi-port bond graph representation [2, 3, 7, 21]. In addition, when the system has linear junction structure and constitutive laws and a single input, the state equations are linear time invariant and have the following general form:

$$\dot{\mathbf{x}} = \mathbf{A}\mathbf{x} + \mathbf{b}u \tag{10.2}$$

where, $\mathbf{A} \in \mathbb{R}^{m\times m}, \mathbf{b} \in \mathbb{R}^m$ are the state space matrices, $\mathbf{x} \in \mathbb{R}^m$ is the state variable vector, $u \in \mathbb{R}$ is the input, and m is the number of independent states.

For the above system appropriate outputs are defined in order to effortlessly calculate the power of each energy element in the model using the constitutive law of each element. For convenience, the outputs are selected to be the generalized flow, effort, and flow for inertial, compliant, and resistive elements, respectively. The dual effort or flow variables needed for calculating the power are derived from the output variables and constitutive laws. The output vector for this set of variables has the form:

$$\mathbf{y} = \begin{Bmatrix} \mathbf{f}_I \\ \mathbf{e}_C \\ \mathbf{f}_R \end{Bmatrix} \tag{10.3}$$

where $\mathbf{y} \in \mathbb{R}^k$ and $\mathbf{f}_I \in \mathbb{R}^{k_I}, \mathbf{e}_C \in \mathbb{R}^{k_C}$, and $\mathbf{f}_R \in \mathbb{R}^{k_R}$. The variables k_I, k_C, and k_R represent the number of inertial, compliant, and resistive elements, respectively. The total number of energy elements is $k = k_I + k_C + k_R$. Note that the output vector is defined such that the required variables of the inertial elements are first followed by the variables of compliant and then resistive elements.

Each output variable is a linear function of the state variables, and possibly input, given that they have linear constitutive laws. Using the output variables set in (10.3), the output equations are written as:

$$\mathbf{y} = \mathbf{C}\mathbf{x} + \mathbf{d}u \tag{10.4}$$

where $\mathbf{C} \in \mathbb{R}^{k\times m}, \mathbf{d} \in \mathbb{R}^k$ are the output state space matrices.

Given this set of output variables the missing efforts or flows, needed for calculating the element power, are computed from the linear constitutive laws of each type of energy element as shown below:

$$\begin{aligned} &\mathbf{I}: \; p_I = r_I f_I \iff e_I = \dot{p}_I = r_I \dot{f}_I \\ &\mathbf{C}: \; q_C = r_C e_C \iff f_C = \dot{q}_C = r_C \dot{e}_C \\ &\mathbf{R}: \; e_R = r_R f_R \end{aligned} \tag{10.5}$$

where r_I, r_C, r_R are known constants representing the linear constitutive law coefficients of inductance, compliance, and resistance, respectively. For deriving compact expressions in the analysis, a vector, $\mathbf{r} \in \mathbb{R}^k$, with all the linear constitutive law coefficients is introduced as shown below:

$$\mathbf{r} = \begin{Bmatrix} \mathbf{r}_I \\ \mathbf{r}_C \\ \mathbf{r}_R \end{Bmatrix} \tag{10.6}$$

where $\mathbf{r}_I \in \mathbb{R}^{k_I}$, $\mathbf{r}_C \in \mathbb{R}^{k_C}$, and $\mathbf{r}_R \in \mathbb{R}^{k_R}$ are the constant constitutive law coefficients.

Finally, the power needed for calculating the activity of each element, as defined in (10.1), is computed as the product of generalized effort and flow. By using (10.5) the following expressions for the power of each element type are derived:

$$\begin{aligned} &\mathbf{I}: \ \mathbb{P}_I = e_I f_I = r_I f_I \dot{f}_I \\ &\mathbf{C}: \ \mathbb{P}_C = e_C f_C = r_C e_C \dot{e}_C \\ &\mathbf{R}: \ \mathbb{P}_R = e_R f_R = r_R f_R f_R = r_R f_R^2 \end{aligned} \tag{10.7}$$

The expressions for element power in (10.7) are generalized with the use of the defined structure of the output vector in (10.3) and parameter vector in (10.6). Thus, the power for energy storage elements (inertial and compliant) is given by (10.8) and for energy dissipation elements (resistive) in (10.9).

$$\mathbb{P}_i = r_i y_i \dot{y}_i, \quad i = 1, \ldots, k_I + k_C \tag{10.8}$$

$$\mathbb{P}_i = r_i y_i^2, \quad i = k_I + k_C + 1, \ldots, k \tag{10.9}$$

The above element power is then used to calculate the element activity based on its definition in (10.1). Element parameters are assumed to be constant thus the activity for the energy storage elements is given in (10.10) and for energy dissipation element in (10.11).

$$A_i = \int_0^\tau |\mathbb{P}_i| = r_i \int_0^\tau \left| y_i \dot{y}_i \right| \mathrm{d}t, \quad i = 1, \ldots, k_I + k_C \tag{10.10}$$

$$A_i = \int_0^\tau |\mathbb{P}_i| = r_i \int_0^\tau \left| y_i^2 \right| \mathrm{d}t = r_i \int_0^\tau y_i^2 \mathrm{d}t, \quad i = k_I + k_C + 1, \ldots, k \tag{10.11}$$

10.2.2 Activity for Single Harmonic Excitation

The time response of the output vector, $\mathbf{y}(t)$, in (10.3) and (10.10) is required in order to complete the calculation of element power. For nonlinear systems, numerical integration is typically used to calculate the system response; however, in this case

linear system analysis can be used to obtain closed form expressions. In addition, for the purposes of this work, the excitation is assumed to be a single harmonic given by:

$$u(t) = U \sin(\omega t) \tag{10.12}$$

where $U \in \mathbb{R}$ is the amplitude of the excitation and ω is the excitation frequency. The steady state response of the linear system in (10.2) and (10.4) under the harmonic excitation in (10.12) is calculated using linear system analysis theory. The response is given by the following closed form expression:

$$y_i(t, \omega) = UY_i(\omega) \cdot \sin(\omega t + \varphi_i(\omega)), \quad i = 1, \ldots, k \tag{10.13}$$

where $Y_i(\omega)$ and $\varphi_i(\omega)$ are the steady state amplitude and phase shift, respectively, that can be easily calculated using linear system analysis.

Within the context of this analysis, the output $y_i(t, \omega)$ in (10.13) is either an effort or a flow that is used for calculating the power of each element in (10.8) and (10.9). Finally, the activity can be calculated by (10.10) and (10.11), but first the upper bound, τ, of this integral must be specified. For this case, the steady state and periodicity features of the response are exploited. A periodic function repeats itself every T seconds, and therefore, a single period of this function contains the necessary information about the response. Thus, the upper bound of the integral is set to one period of the excitation, $\tau = T = 2\pi/\omega$. Therefore, the steady state activity for energy storage elements is given by:

$$\begin{aligned} A_i^{\text{ss}}(\omega) &= r_i \int_0^T \left| y_i \dot{y}_i \right| \mathrm{d}t \\ &= \frac{1}{2} r_i U^2 Y_i^2(\omega)\, \omega \int_0^T \left| \sin(2(\omega t + \varphi_i(\omega))) \right| \mathrm{d}t \\ &\Rightarrow A_i^{\text{ss}}(\omega) = 2 r_i U^2 Y_i^2(\omega) \end{aligned} \tag{10.14}$$

and for energy dissipation elements by:

$$\begin{aligned} A_i^{\text{ss}}(\omega) &= r_i \int_0^T y_i^2 \mathrm{d}t \\ &= r_i U^2 Y_i^2(\omega) \int_0^T \sin^2(\omega t + \varphi_i(\omega)) \mathrm{d}t \\ &\Rightarrow A_i^{\text{ss}}(\omega) = \frac{\pi r_i U^2 Y_i^2(\omega)}{\omega} \end{aligned} \tag{10.15}$$

The above simple closed form expressions can be used to calculate the activity of energy elements for a given single harmonic excitation. These expressions are proportional to the square of the amplitude; however, they have no dependency on the phase shift that is eliminated through the integration. The superscript "ss" in

(10.14) and (10.15) denotes the activity under a steady state harmonic response. Note that the activity for both energy storage and energy dissipation elements is a function of the excitation frequency but not the phase shift.

10.2.3 Activity Index and MORA

The activity as defined in (10.1) is a measure of the absolute importance of an element as it represents the amount of energy that flows through the element over a given time period. In order to obtain a relative measure of the importance, the element activity is compared to a quantity that represents the "overall activity" of the system. This "overall activity" is defined as the sum of all the element activities of the system, is termed total activity (A^{Total}), and is given by:

$$A^{\text{Total}}(\omega) = \sum_{i=1}^{k} A_i(\omega) \tag{10.16}$$

where A_i is the activity of the ith element given by (10.14) and (10.15). Thus a normalized measure of element importance, called element activity index or just activity index, is defined as:

$$\text{AI}_i^{\text{ss}}(\omega) = \frac{A_i^{\text{ss}}(\omega)}{A^{\text{Total}}(\omega)} = \frac{A_i^{\text{ss}}(\omega)}{\sum_{i=1}^{k} A_i^{\text{ss}}(\omega)} \tag{10.17}$$

The activity index, $\text{AI}_i^{\text{ss}}(\omega)$, is calculated for each element in the model and it represents the portion of the total system energy that flows through a specific element. The input amplitude, U, does not appear in any of the element activity indices since all element activities are proportional to the square of the amplitude.

With the activity index defined as a relative metric for addressing element importance, the Model Order Reduction Algorithm (MORA) is constructed. The first step of MORA is to calculate the activity index for each element in the system as defined in (10.17). Next, the activity indices are sorted to identify the elements with high activity (most important) and low activity (least important). With the activity indices sorted, the model reduction proceeds given the desired engineering specifications. These specifications are defined by the modeler who then converts them into a threshold β of the total activity (e.g., 99 %) that he or she wants to include in the reduced model. This threshold defines the borderline between the eliminated and retained elements in the model. The elimination process is shown in Fig. 10.1 where the sorted activity indices are summed starting from the most important element until the specified threshold is reached. The element which, when included, increments the cumulative activity index above the threshold, is the last element to be included in the reduced model. The elements that are above this threshold are removed from the model, e.g., when using the bond graph formulation,

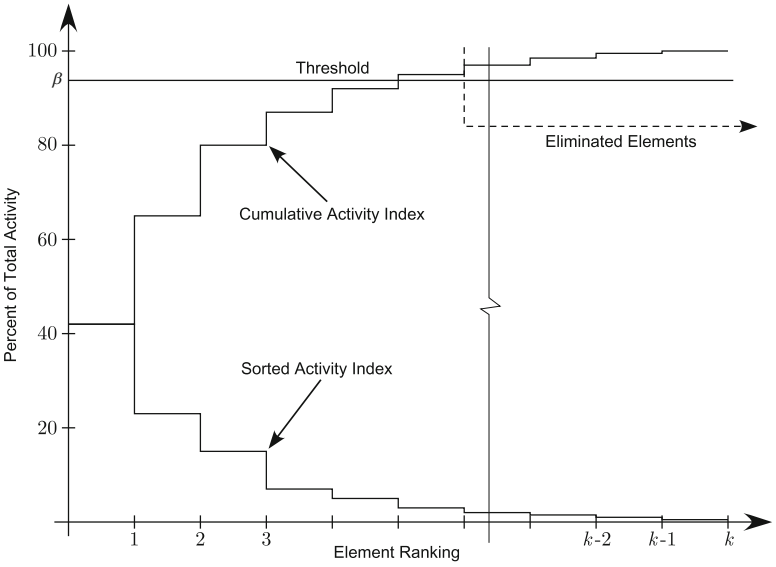

Fig. 10.1 Activity index sorting and elimination

delete the corresponding low activity energy element. The junction structure of the bond graph is retained in the reduced model, and therefore, the reduced model realization is the same as the full model, so its physical meaning and relation to the physical system are retained.

10.3 Cantilever Beam Model

The state space model used in the previous section assumes a lumped parameter system representation, where individual components exhibit only inertial, compliant, or resistive behavior. This means that the dynamic behavior of a component can be lumped and modeled as a single inertial, compliant, or resistive energy element. This can be a valid assumption for many components; however, real system components can possess all dynamic properties (inertial, compliant, and resistive) simultaneously. In addition, these properties may vary or be distributed spatially. In these cases, a lumped parameter modeling approach cannot be used since it will result in an incorrect model and produce inaccurate predictions. An example of such component is a beam and more specifically a cantilever beam that is widely used in engineering applications. Therefore, these components must be considered as distributed parameter or continuous, which require a different modeling approach.

Models of continuous systems are developed using solid mechanics theory, which instead of Ordinary Differential Equations, lead to Partial Differential

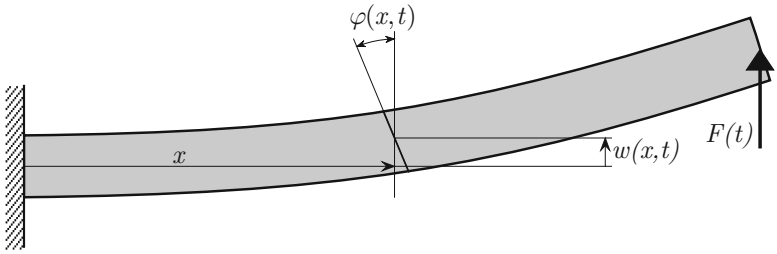

Fig. 10.2 Cantilever beam transverse vibration

Equations (PDE) with derivatives in both space and time [1, 6, 8, 23]. The continuous cantilever beam used in this work is shown in Fig. 10.2, where its transverse motion is considered when excited by a vertical load at its free end. The motion of a given gross section, $w(x, t)$ and $\varphi(x, t)$, from its undeformed state varies with time and location thus having a set of PDEs describing its motion. Note that due to the rotation φ, a cross section does not remain normal to the neutral axis according to the Timoshenko beam theory. One method for solving these PDEs is separation of variables, which produces a modal expansion solution [18]. This approach can also be combined with other lumped parameter elements in order to model a real system that consists of both lumped and distributed parameter components [7]. An analysis of the advantages and disadvantages of this approach is beyond the scope of this work, however, it is safe to say that the solution of PDEs is more cumbersome than the solution of ordinary differential equations that describe the behavior of lumped parameters system.

A different approach for modeling the transverse vibration of a cantilever beam is to divide it into segments of equal length. This approach is motivated by the procedure for deriving the PDEs describing the motion of a beam. Each of these segments has linear inertial and compliant properties that can be determined from solid mechanics theory. Shear effects and rotational inertial effects are also considered, which results in a more generic model that is valid for a larger range of geometric parameters. This is known as the Timoshenko beam model, which is usually used for non-slender beams in order to get accurate model predictions. The use of this more complex model using the Timoshenko beam theory is also mandated from the use of MORA in the process of determining the appropriate model complexity. In this approach the most complex model is first developed, and then MORA is used to identify what is actually needed in order to reach a reduced model with accurate predictions.

The ideal physical model of a cantilever beam under these assumptions is shown in Fig. 10.3 where the beam is divided into n equal segments. This model approaches the partial differential equations of the continuous system, as the number of segments approaches infinity. However, it is difficult to predict the number of segments required to achieve a given level of accuracy. It is well known that a large number of segments are required for accurately predicting low frequency dynamics.

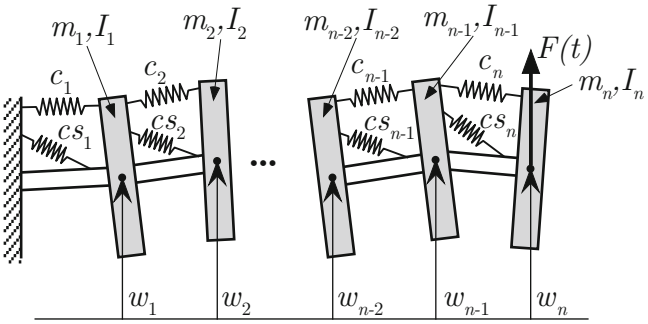

Fig. 10.3 Ideal physical model of a Timoshenko beam

For the purposes of this work the number of segments is chosen based on previous research, such that the model accurately predicts low frequency dynamics that are considered in this work [11, 12]. With the given number of segments, the physical phenomena to be included in each segment, for the model to accurately predict the dynamic behavior, will then be identified using the proposed methodology in this chapter.

For calculating the constitutive law parameters of the energy storage elements, the beam is assumed to have density ρ, Young's modulus E, shear modulus G, length L, cross sectional area A, and cross sectional moment of inertia I. Given these physical parameters of the beam, the element parameters in the above linear model are given by the expressions below:

$$\begin{aligned} m_i &= \rho A \Delta x, \quad i = 1, \ldots, n \\ I_i &= \rho I \Delta x, \\ c_i &= \tfrac{\Delta x}{EI} \\ cs_i &= \tfrac{\Delta x}{\kappa G A} \end{aligned} \tag{10.18}$$

where $\Delta x = L/n$ is the length of each segment, κ is a dimensionless constant that accounts for the non-uniform distribution of the shear stress and depends on the shape of the cross section. The inertial parameters m_i and I_i represent the linear and rotational inertia of each segment, respectively. The parameters c_i and cs_i represent the bending and shear compliance between two segments, respectively. The beam is assumed to have no energy losses therefore there are no damping elements in the model. These parameters are used to define the parameter vector as defined in (10.6).

For developing the dynamic equations, the bond graph formulation is used. Bond graphs provide the power topography of the system and it is a natural selection for implementing the power-based activity metric. The bond graph model of the ideal physical model as shown in Fig. 10.3 is developed and given in Fig. 10.4. The bond graph has $4n$ independent state variables since each segment is modeled by four independent energy storage elements and the state vector has the form $\mathbf{x} = \{p_1, \ldots, p_n, p_{I1}, \ldots, p_{In}, q_1, \ldots, q_n, q_{s1}, \ldots, q_{sn}\}^T$. The variable p represents the momentum of inertial elements and q the displacement of compliant elements. The velocity of the each mass, v_i, represents the transverse velocity at a given location of the continuous beam and (10.19) expresses the relation between the

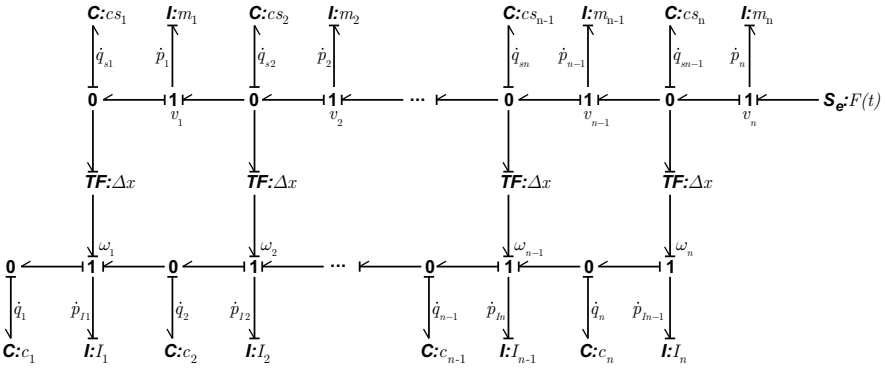

Fig. 10.4 Bond graph model of a Timoshenko beam

discrete and continuous variables. The other kinematic variable of the model, ω_i, is the rotation at a given location and its relation to the continuous variable is given in (10.20).

$$v_i(t) = \dot{w}_i = \dot{w}\left(i\Delta x, t\right) \tag{10.19}$$

$$\omega_i(t) = \dot{\varphi}_i = \dot{\varphi}\left(i\Delta x, t\right) \tag{10.20}$$

The state and output equations in matrix form are derived using the multi-port approach, which provides easy derivations of the state matrices [20]. According to this approach, most of the junction structure matrices are zero, and the state space and input matrices are given by:

$$\mathbf{A} = \mathbf{J}_{\mathrm{SS}}\,\mathbf{S}, \quad \mathbf{b} = \mathbf{J}_{\mathrm{SU}} \tag{10.21}$$

where $\mathbf{S} \in \mathbb{R}^{4n\times 4n}$ is a diagonal matrix with the inertial and compliant parameters of each element, and $\mathbf{J}_{\mathrm{SS}} \in \mathbb{R}^{4n\times 4n}$, $\mathbf{J}_{\mathrm{SU}} \in \mathbb{R}^{4n}$ are the junction structure matrices describing the interconnections between the energy elements, and they are given in the Appendix.

The output vector as define in the previous section in (10.3) becomes $\mathbf{y} = \{f_1, \ldots, f_{2n}, e_1, \ldots, e_{2n}\}^T$. Thus, the output matrices as defined in (10.4), which are required for calculating the power flow into the energy elements, are given by:

$$\mathbf{C} = \mathbf{S}, \quad \mathbf{d} = \mathbf{0} \tag{10.22}$$

The dimensions of the state space matrices as defined in the previous section are $m = 4n$ and $k = 4n$.

For the above model with n segments the steady state response is first calculated using (10.13) and based on the state space equations in (10.21) and (10.22). Then the element activity is calculated from (10.14), which gives the following expression for the energy storage elements of the model:

$$A_i^{\mathrm{ss}}(\omega) = 2r_i U^2 Y_i^2(\omega), \quad i = 1, \ldots, 4n \tag{10.23}$$

The above analysis enables the calculation of the element activity for a given single harmonic excitation. The activity index that is used by MORA is independent of the excitation amplitude, as shown in (10.17), and therefore can be set to an arbitrary value, e.g., set to one (1) for simplicity. Model complexity and which physical phenomena need to be included, can be determined given the element activity in (10.23) and MORA. The complexity of the beam is investigated in the next section in order to identify the significant elements based on beam length and element location. A series of analysis is performed in order to get more insight into the important beam dynamics under different scenarios.

10.4 Beam Complexity Based on Activity

The activity metric and MORA is applied to a steel cantilever beam with parameters $\rho = 7860$ kg/m^3, $E = 210$ GPa, $G = 80$ GPa, $A = 3 \times 10^{-3}$ m^2, $I = 2.5 \times 10^{-6}$ m^4, $\kappa = 0.85$. The length of the beam is varied, $L = 0.2$–2.0 m, in order to study the variation of element significance. The methodology is easy and computationally inexpensive to implement due to the simple and closed form expressions used for calculating the state space matrices, frequency response, and activity.

First, the beam length is set to 2.0 m such that the beam is considered to be slender. The number of segments is set to $n = 30$ and therefore there are a total of 120 energy storage elements modeling the beam. In this case the modeling target is set to accurately predict static behavior of low frequency dynamics, thus, the excitation frequency is set to 95 % of the first natural frequency (122.7 rad/s).

The results of the activity analysis using (10.23) and under these assumptions are shown in Fig. 10.5 where the activity index of all 120 elements is shown. Element numbers 1–30 represent the activity index of the linear inertia (m_i) and 31–60 the activity index of the rotational inertia (I_i) of each segment. Next, element numbers 61–90 and 91–120 represent the activity index of the bending (c_i) and shear ($\mathrm{cs_i}$) compliance, respectively. For each range of elements the smallest numbers represent elements that are next to the fixed end of the beam. It is clear from the activity analysis that the most important elements are related to the linear inertia and the bending stiffness of the beam. On the contrary, the elements related with the rotary inertia and shear stiffness have very low activity and thus are insignificant under these conditions. This initial activity analysis agrees with common practice, in which a slender beam is modeled using the Euler–Bernoulli theory that neglects rotational inertia and shear stress effects.

Model complexity is systematically addressed using MORA as it is described in Sect. 10.2.3. Elements are ranked according to their activity index as shown in Fig. 10.6 where the sorted activity indices along with the cumulative activity index are plotted. According to the activity analysis, 40 of the 120 elements account for almost 99 % of the energy flows through the model. This is a significant result verifying that unnecessary complexity is included in the model; however, the figure does not directly depicts the elements that are insignificant and could be eliminated from the model.

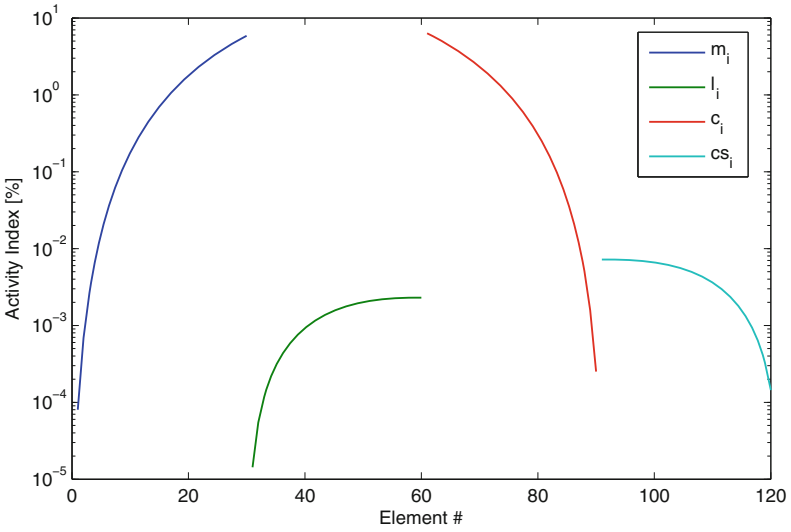

Fig. 10.5 Element activity indices for slender beam

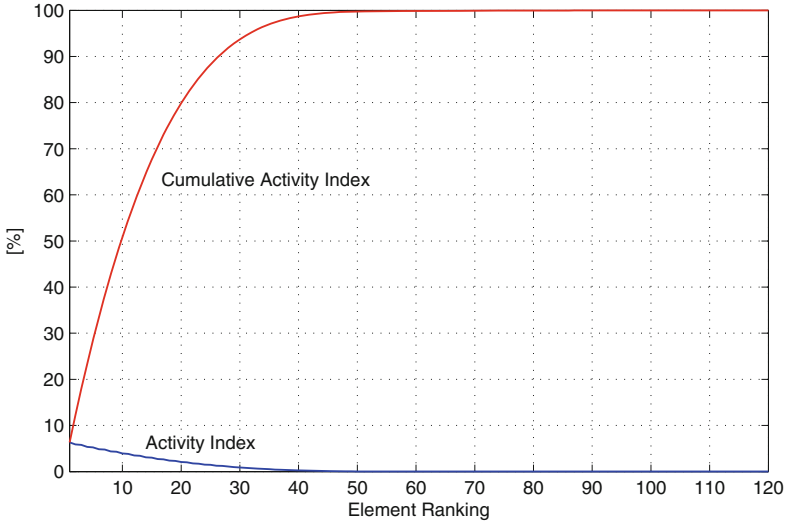

Fig. 10.6 Element ranking for slender beam

The important elements are next identified using MORA. Using a reduction threshold, $\beta = 99.5\ \%$, MORA identifies the elements that have a significant contribution to the system dynamic behavior. The results of this analysis are shown in Fig. 10.7 where both the activity and elimination/inclusion in the reduced model are depicted. The "+" symbol identifies the elements with significant contribution and must be included, where the "o" symbol identifies that an element

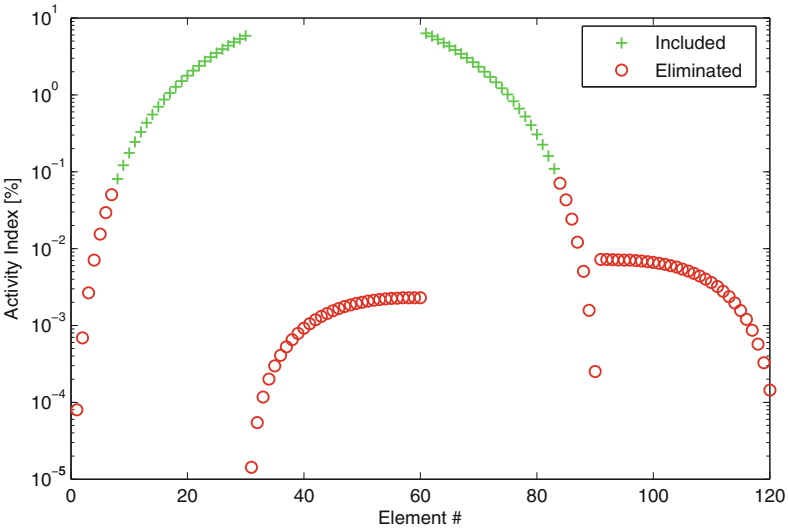

Fig. 10.7 Model reduction for slender beam, $L = 2$ m

is insignificant and must be eliminated from the full model in order to generate the reduced model. Out of the 120 elements only 46 are important and the remaining 74 can be eliminated. More specifically, MORA identifies that all rotational inertia and shear stiffness elements must be eliminated from the model. Linear inertia elements that are close to the support have low activity and can be eliminated from the model, where inertial elements towards the free end of the beam have high activity and must be retained. The reverse is true for the bending stiffness elements, where the elements towards the free end can be eliminated and the ones near the support must be retained. More specifically, 23 of the linear inertia and 23 of the bending stiffness elements have high activity and must be included in the reduced model.

The same reduction using MORA is performed with different beam lengths in order to study how element importance changes as the length is reduced. The reduction for a beam length of 0.7 m is shown in Fig. 10.8. The same trend is observed for the elimination of linear inertia and bending stiffness elements. The activity index of all rotational inertia elements (31–60) is higher than before ($L = 2$ m) but still very low, and therefore, they are eliminated from the model. The activity of shear stiffness (91–120) also increases and some of these elements become important. The shear stiffness elements that are close to the support have higher activity index and have to be included in the reduced model, while the ones towards the free end are eliminated. A total of 71 elements are included in the reduced model with 25 linear inertia, 25 bending stiffness, and 21 shear stiffness elements.

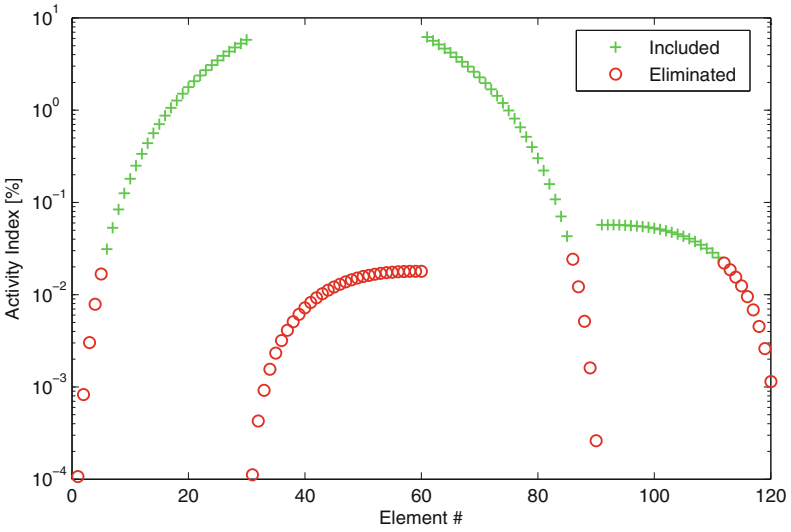

Fig. 10.8 Model reduction for $L = 0.7$ m

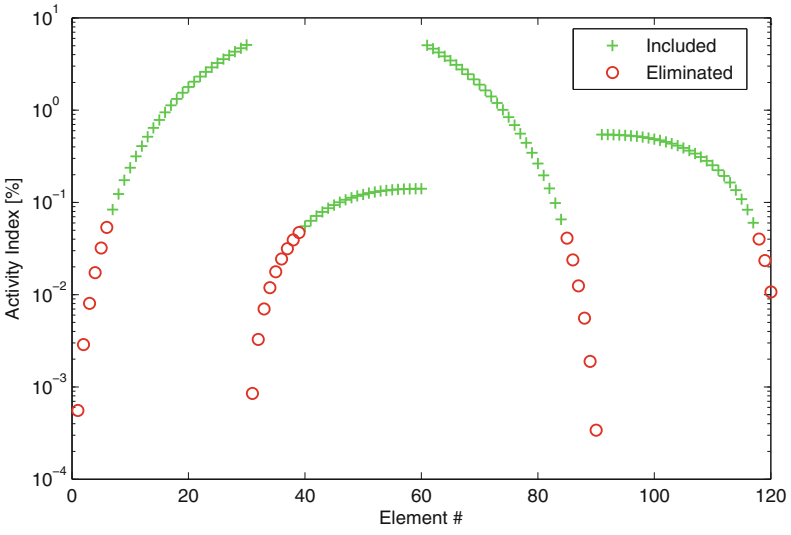

Fig. 10.9 Model reduction for $L = 0.2$ m

The beam length is further reduced to 0.2 m in order to examine if more elements become important. The activity index of the linear inertia and bending stiffness remains almost unchanged as shown in Fig. 10.9. However, the activity index of the rotational inertia and shear stiffness is further increased such that some of the rotational inertia elements also become important. More specifically the rotational

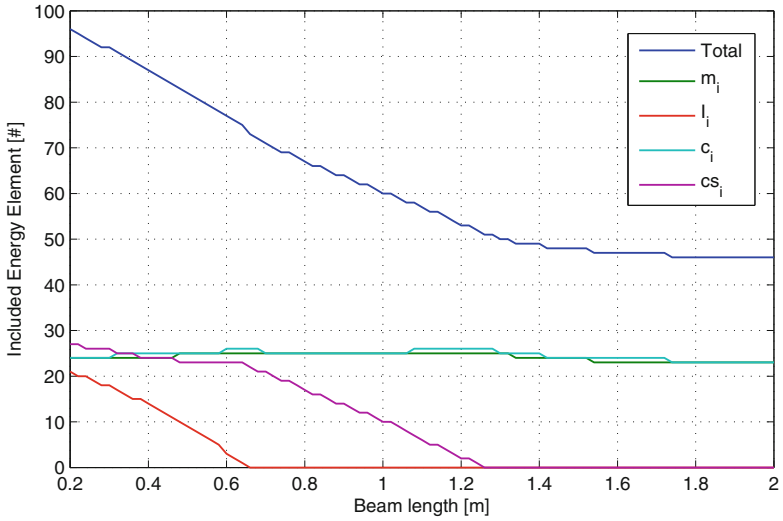

Fig. 10.10 Model reduction for length variation

inertia elements that are towards the free end are important and the ones near the fixed end are eliminated. A total of 96 elements out of 120 are included in the reduced model with 24 linear inertia, 21 rotational inertia, 24 bending stiffness, and 27 shear stiffness elements.

The variation of beam length showed that the total number of important elements increases as the beam length decreases. This variation is investigated in more detail by varying the beam length from 0.2 to 2 m with a step of 20 mm. The number of included linear and rotational inertia, and bending and shear stiffness is recorded along with the total number of elements. The results of this analysis are shown in Fig. 10.10. The total number of elements is monotonically increasing as the beam length is decreased. The number of linear inertia and bending stiffness remains almost constant as the length changes. On the contrary, the number of shear stiffness elements is zero until about 1.2 m where it becomes important and starts increasing. Further reduction in length results in a monotonic increase in the number of included shear stiffness element. A similar behavior is observed for the number of the rotational inertia elements; however, they become important at a lower beam length of about 0.6 m.

The validity of the generated reduced models is verified by analyzing the accuracy of the model. Specifically the steady state response amplitude for the velocity at the free end and the torque at the fixed end are calculated. The comparison is made with the corresponding response of the full model and over the range of beam lengths used before. The accuracy for both variables, as shown in Fig. 10.11, varies as the beam length is changed, with averages around 91.5 %. The discrete variation in accuracy is due to the change of model complexity as different elements are added or removed in the reduced model according to the activity metric.

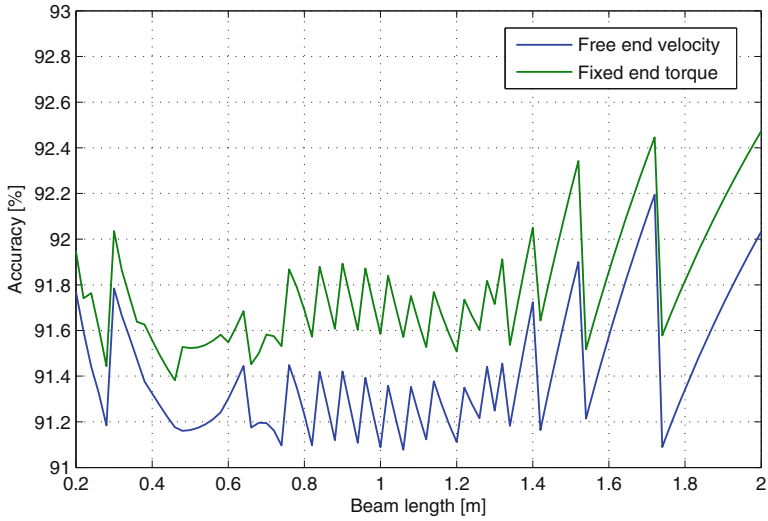

Fig. 10.11 Model accuracy

Next, a similar experiment is performed with the same conditions except the excitation frequency, which is increased to 95 % of the second natural frequency and more specifically at 722.8 rad/s. Given that the number of segments remains the same, it is expected that the number of important elements will increase. This is a known feature of finite segment models that require an increased number of segments in order to accurately predict higher frequency dynamics. Model reduction and identification of significant dynamics is performed for a slender beam ($L = 2.0$ m). The results of the activity analysis are shown in Fig. 10.12 and in general a higher number of elements are required in order to achieve a similar level of accuracy. Again, some elements at the ends of the beam can be eliminated due to their low activity. Another general observation is that low activity elements appear also within the span of the beam, in addition to the ones at the ends of the beam. The drop in activity appears around the nodes of the second mode where there is a stationary point. For example, for the linear inertia there is one very low activity element that coincides with the node of the second transverse vibration mode. Similar behavior is observed for the other energy elements as shown in Fig. 10.12. More specifically a total of 68 elements out of 120 are included in the reduced model with 27 linear inertia, two rotational inertia, 28 bending stiffness, and 11 shear stiffness elements. Similar reduction patterns, as with the excitation near the first mode, are observed for various beam lengths but not shown here for brevity.

The effect of beam length on element importance is studied next by varying the beam length ($L = 0.2 - 2.0$ m) and performing model reduction using MORA. The results of this analysis are shown in Fig. 10.13 where the number of each type of element, that needs to be included in the reduced model, is shown as a function of the beam length. The number of important linear inertia and bending stiffness elements is remains almost constant as the beam length is varied. On the contrary,

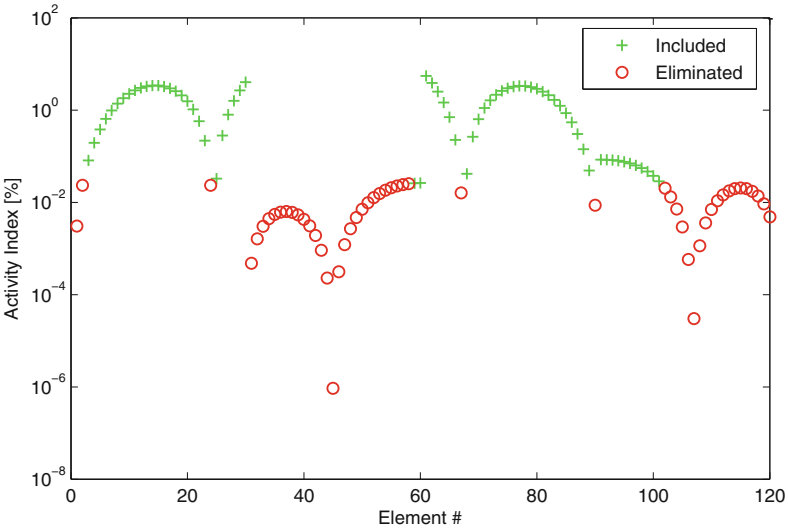

Fig. 10.12 Model reduction for slender beam, excitation near second mode, $L = 2.0$ m

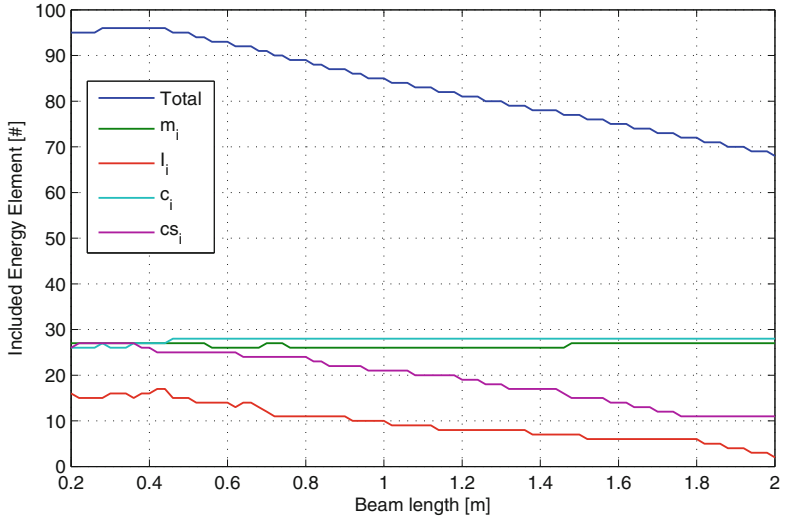

Fig. 10.13 Model reduction for length variation, excitation near second mode

the number of rotational inertia and shear stiffness elements reduces as the length of the beam increases, in accordance with the Timoshenko beam theory. However, rotational inertia and shear stiffness elements are important and have to be included in the reduced model even when the beam is slender, i.e., $L = 2.0$ m. The total number of important elements is overall higher, as compared to the total number of elements when the excitation is near the first natural frequency.

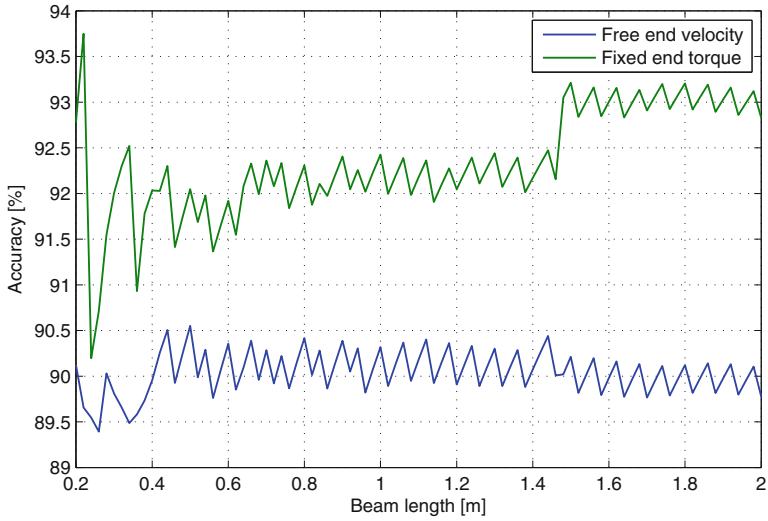

Fig. 10.14 Reduced model accuracy, excitation near second mode

The accuracy of the reduced model is also calculated for the linear velocity at the free end and the torque at the fixed end (Fig. 10.14). The comparison is made with the initial full model that includes all elements, i.e., 30 segments and 120 energy storage elements. The two variables have similar accuracy throughout the whole range of beam lengths. Also, the overall accuracy of there reduced models is similar to the accuracy of the reduced models when the excitation is near the first natural frequency.

10.5 Discussion and Conclusions

A new methodology is developed that reduces the complexity of a Timoshenko or Euler–Bernoulli beam model, by providing more insight into the beam dynamic behavior at the same time. The proposed methodology provides a systematic modeling procedure for cantilever beams that are modeled through the finite segment approach. The previously developed activity metric is used as the basis for determining the physical phenomena that need to be included in each segment in order for a reduced model to accurately predict the dynamic behavior of a beam. The procedure starts with the most complicated model, Timoshenko in this case, and then eliminates insignificant elements that do not contribute to the dynamic behavior according to the activity metric.

The results presented in this work are in agreement with the assumptions of beam theories, which suggest that the Timoshenko beam model must be used for shorter rather than slender beams. The proposed methodology can be used when modeling beams, in order to decide which of the two models to use, Timoshenko or Euler–Bernoulli. In addition, the activity metric can refine the modeling assumptions by identifying what physical phenomena need to be included in each segment, i.e., linear and rotational inertia, bending and shear stiffness. This results in a non-uniform reduced model where different physical phenomena are included along the length of the beam.

The number of segments is a significant parameter when it comes to modeling using the finite segment approach but it was considered constant in the analysis of the presented results. The methodology was also performed with various, lower and higher, number of segments; however, these results are not presented in this chapter for brevity. The reduced models for different number of segments are identical with the ones presented in this work as shown in Fig. 10.10. The only difference is the actual number of included elements; however, the ratio of included elements to the total number of elements remains the same.

The activity analysis is performed for two excitation frequencies that are around the first and second natural frequencies. These excitations are chosen by making the assumption that the model will be used with low frequency excitations. The analysis showed that a higher number of elements are needed as the excitation frequency increases; however, the overall accuracy of the reduced model remains the same. A similar analysis can be performed for even higher excitation frequencies or range of frequencies in order to account for more realistic excitations. However, this procedure has to be formalized and this remains as an item for future research.

Because this work uses an energy-based modeling metric, it is convenient to use a model representation and formulation approach from which energy can be easily extracted/calculated. The bond graph approach explicitly represents the power topography of a dynamic system, and therefore, it is used in this work for calculating the necessary variables required for the power calculations. To be clear, the use of this methodology is not limited to systems represented by bond graphs. It can also be applied when the continuous system is modeled using any other modeling methodology, e.g., Lagrange's equations, Newton's Law, etc. However, in this case the calculation of power that is required for the proposed methodology might not be as trivial as using the bond graph formulation.

The activity metric effectively addresses the model complexity of distributed parameter components and in addition provides physical insight into the model. The results of this chapter provide more insight into the nature of the reduced models produced by MORA, and therefore, demonstrate that MORA is an even more useful tool than previously realized for the production of proper models of nonlinear systems.

Appendix: Junction Structure Matrices

$$\mathbf{S} = \begin{bmatrix} m_i\,\mathbf{I}_{n\times n} & \mathbf{0}_{n\times n} & \mathbf{0}_{n\times n} & \mathbf{0}_{n\times n} \\ \mathbf{0}_{n\times n} & I_i\,\mathbf{I}_{n\times n} & \mathbf{0}_{n\times n} & \mathbf{0}_{n\times n} \\ \mathbf{0}_{n\times n} & \mathbf{0}_{n\times n} & c_i\,\mathbf{I}_{n\times n} & \mathbf{0}_{n\times n} \\ \mathbf{0}_{n\times n} & \mathbf{0}_{n\times n} & \mathbf{0}_{n\times n} & \mathrm{cs}_i\,\mathbf{I}_{n\times n} \end{bmatrix}^{-1}$$

$$\mathbf{J}_{SS} = \begin{bmatrix} \mathbf{0}_{n\times n} & \mathbf{0}_{n\times n} & \mathbf{0}_{n\times n} & \mathbf{J}_1 \\ \mathbf{0}_{n\times n} & \mathbf{0}_{n\times n} & \mathbf{J}_1 & \Delta x\,\mathbf{I}_{n\times n} \\ \mathbf{0}_{n\times n} & -\mathbf{J}_1^T & \mathbf{0}_{n\times n} & \mathbf{0}_{n\times n} \\ -\mathbf{J}_1^T & -\Delta x\,\mathbf{I}_{n\times n} & \mathbf{0}_{n\times n} & \mathbf{0}_{n\times n} \end{bmatrix}$$

$$\mathbf{J}_{SU} = \begin{Bmatrix} \mathbf{0}_{(n-1)\times 1} \\ 1 \\ \mathbf{0}_{3n\times 1} \end{Bmatrix}$$

$$\mathbf{J}_1 = \begin{bmatrix} -1 & 1 & 0 & 0 & \dots & 0 & 0 & 0 \\ 0 & -1 & 1 & 0 & \dots & 0 & 0 & 0 \\ 0 & 0 & -1 & 1 & \dots & 0 & 0 & 0 \\ \vdots & \vdots & \vdots & \vdots & \ddots & \vdots & \vdots & \vdots \\ 0 & 0 & 0 & 0 & \dots & -1 & 1 & 0 \\ 0 & 0 & 0 & 0 & \dots & 0 & -1 & 1 \\ 0 & 0 & 0 & 0 & \dots & 0 & 0 & -1 \end{bmatrix}$$

References

1. Bauchau, O. A., & Craig, J. I. (2009). *Structural analysis*. Berlin: Springer. ISBN 978-90-481-2515-9.
2. Borutzky, W. (2004). *Bond graph methodology: Development and analysis of multidisciplinary dynamic systems*. Berlin: Springer. ISBN 978–1848828810.
3. Brown, F. T. (2006). *Engineering system dynamics: A unified graph-centered approach* (2nd ed.). Boca Raton, FL: CRC Press. ISBN 9780849396489.
4. Ferris, J. B., & Stein, J. L. (1995). Development of proper models of hybrid systems: A bond graph formulation. *Proceedings of the 1995 International Conference on Bond Graph Modeling* (pp. 43–48), January, Las Vegas, NV. Published by SCS, ISBN 1-56555-037-4, San Diego, CA.

5. Ferris, J. B., Stein, J. L., & Bernitsas, M. M. (1998). Development of proper models of hybrid systems. *Transactions of the ASME, Journal of Dynamic Systems, Measurement, and Control, 120*(3), 328–333.
6. Genta, G. (2009). *Vibration dynamics and control*. Dordrecht: Springer. ISBN 978-0-387-79579-9.
7. Karnopp, D. C., Margolis, D. L., & Rosenberg, R. C. (2006). *System dynamics: Modeling and simulation of mechatronic systems* (4th ed.). New York: Wiley. ISBN 978-0-471-70965-7.
8. Li, X. F. (2008). A unified approach for analyzing static and dynamic behaviors of functionally graded Timoshenko and Euler–Bernoulli beams. *Journal of Sound and Vibration, 318*(4–5), 1210–1229.
9. Li, D. F., & Gunter, E. J. (1981). Study of the modal truncation error in the component mode analysis of a dual-rotor. *Transactions of the ASME, Journal of Engineering for Gas Turbines and Power, 104*(3), 525–532.
10. Liu, D.-C., Chung, H.-L., & Chang, W.-M. (2000). Errors caused by modal truncation in structure dynamic analysis. *Proceedings of the International Modal Analysis Conference—IMAC*, v 2 (pp. 1455–1460). Bethel, CT: Published by Society for Experimental Mechanics Inc., ISSN 1046–6770.
11. Louca, L. S. (2014). Complexity of distributed parameter bond graph models. *Proceedings of the 11th International Conference on Bond Graph Modeling and Simulation—ICGBM'2012* (pp. 789–797), Monterey, CA, USA. San Diego, CA: Published by the Society for Computer Simulation International.
12. Louca, L. S. (2015). Finite segment model complexity of an Euler-Bernoulli beam. *Proceedings of the 8th International Conference on Mathematical Modeling* (pp. 334–340). Vienna, Austria: Published by the International Federation of Automatic Control-IFAC.
13. Louca, L. S., Rideout, D. G., Stein, J. L., & Hulbert, G. M. (2004). Generating proper dynamic models for truck mobility and handling. *International Journal of Heavy Vehicle Systems (Special Issue on Advances in Ground Vehicle Simulation), 11*(3/4), 209–236. Published by Inderscience Enterprises Ltd., ISSN 1744−232X, St. Helier, United Kingdom.
14. Louca, L. S., & Stein, J. L. (2002). Ideal physical element representation from reduced bond graphs. *Journal of Systems and Control Engineering, 216*(1), 73–83. Published by the Professional Engineering Publishing, ISSN 0959–6518, Suffolk, United Kingdom.
15. Louca, L. S., & Stein, J. L. (2009). Energy-based model reduction of linear systems. *Proceedings of the 6th International Symposium on Mathematical Modeling*, Vienna, Austria. Published in the series ARGESIM-Reports No. 35, ISBN 978-3-901608-35-3, Vienna, Austria.
16. Louca, L. S., Stein, J. L., Hulbert, G. M., & Sprague, J. K. (1997). Proper model generation: An energy-based methodology. *Proceedings of the 1997 International Conference on Bond Graph Modeling* (pp. 44–49), Phoenix, AZ. Published by SCS, ISBN 1-56555-103-6, San Diego, CA.
17. Louca, L. S., Stein, J. L., & Hulbert, G. M. (2010). Energy-based model reduction methodology for automated modeling. *Journal of Dynamic Systems Measurement and Control, 132*(6), 061202 (16 pages). Published by the American Society of Mechanical Engineers, ISSN Print 0022–0434, ISSN Online 1528–9028, New York, NY.
18. Meirovitch, L. (1967). *Analytical methods in vibrations*. New York, NY: Macmillan Publishing Inc.
19. Rideout, D. G., Stein, J. L., & Louca, L. S. (2007). Systematic identification of decoupling in dynamic system models. *Journal of Dynamic Systems Measurement and Control, 129*(4), 503–513. Published by the American Society of Mechanical Engineers, ISSN Print 0022–0434, ISSN Online 1528–9028, New York, NY.
20. Rosenberg, R. C. (1971). State-space formulation for bond graph models of multiport systems. *Transactions of the ASME, Journal of Dynamic Systems, Measurement, and Control, 93*, 36–40.
21. Rosenberg, R. C., & Karnopp, D. C. (1983). *Introduction to physical system dynamics*. New York: McGraw-Hill. ISBN 0070539057.
22. Stein, J. L., & Louca, L. S. (1996). A template-based modeling approach for system design: Theory and implementation. *Transactions of the Society for Computer Simulation International*. San Diego, CA: Society for Computer Simulation International. Published by SCS, ISSN 0740-6797/96.

23. van Rensburg, N. F. J., & van der Merwe, A. J. (2006). Natural frequencies and modes of a Timoshenko beam. *Wave Motion, 44*(1), 58–69.
24. Walker, D. G., Stein, J. L., & Ulsoy, A. G. (1996). An input–output criterion for linear model deduction. *Transactions of the ASME, Journal of Dynamic Systems, Measurement, and Control, 122*(3), 507–513.
25. Wilson, B. H., & Stein, J. L. (1995). An algorithm for obtaining proper models of distributed and discrete systems. *Transactions of the ASME, Journal of Dynamic Systems, Measurement, and Control, 117*(4), 534–540.